

Supplementary Materials for

Erythrocyte-Driven Immunization via Biomimicry of their Natural Antigen Presenting Function

Anvay Ukidve^{1, 2, †}, Zongmin Zhao^{1, 2, †}, Alexandra Fehnel¹, Vinu Krishnan^{1, 2}, Daniel C. Pan^{1, 2}, Yongsheng Gao^{1, 2}, Abhirup Mandal^{1, 2}, Vladimir Muzykantov³, Samir Mitragotri^{1, 2, *}

1. John A. Paulson School of Engineering and Applied Sciences, Harvard University, Cambridge, MA 02138, USA.

2. Wyss Institute of Biologically Inspired Engineering at Harvard University, Boston, MA 02115, USA.

3. Department of Systems Pharmacology and Translational Therapeutics and Center for Translational Targeted Therapeutics and Nanomedicine, Perelman School of Medicine, University of Pennsylvania, Philadelphia, PA 19104, USA.

* Corresponding author. **Email:** mitragotri@seas.harvard.edu

† Both authors contributed equally to this work.

Table S1. Physicochemical properties of different particle combinations

Particle	Size (nm) *	Polydispersity (PDI)*	Zeta potential (mV)*
PS-OVA-500	540.93 ± 13.03	0.072 ± 0.031	-21.5 ± 0.1
PLGA-OVA-200	155.73 ± 1.03	0.064 ± 0.033	-21.26 ± 0.2
PS-KLH-200	261.43 ± 2.98	0.073 ± 0.01	-3.08 ± 0.21

* Data presented as mean ± s.e.m.

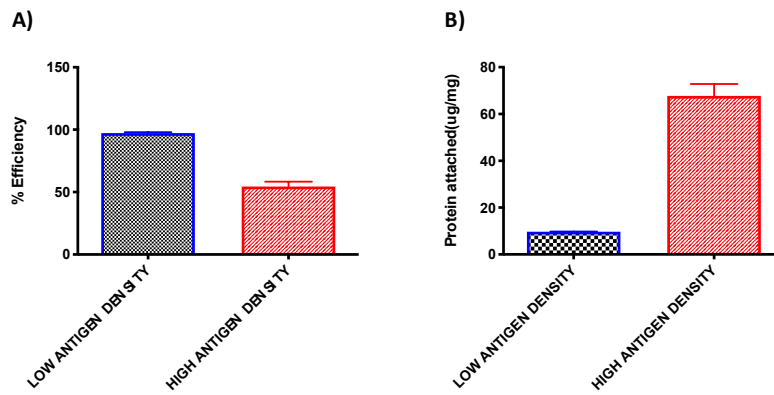


Fig. S1. Attachment of different amount of proteins on the surface of 200 nm polystyrene carboxylate nanoparticles. (A) Attachment efficiency of protein to the PS-COOH. **(B)** Amount of protein attached to PS-COOH expressed in terms of μg attached per mg of particles. Data expressed as mean \pm s.e.m.

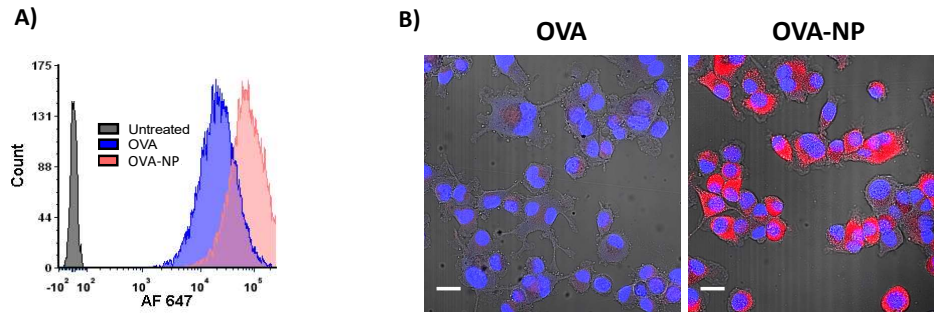


Fig. S2. Internalization of OVA-NP by dendritic cells. (A) Flow cytometry images of dendritic cells post internalization of Alexa Fluor 647 labelled ovalbumin, either in free form (blue) or attached to PS-COOH (red). **(B)** Confocal light scanning micrographs (CLSM) of dendritic cells post internalization of Alexa Fluor 647 labelled ovalbumin either in free form or attached to PS-COOH. Scale bar: 10 μ m. Blue indicates cell nuclei stained with DAPI. Red indicates Alexa Fluor 647 labelled ovalbumin.

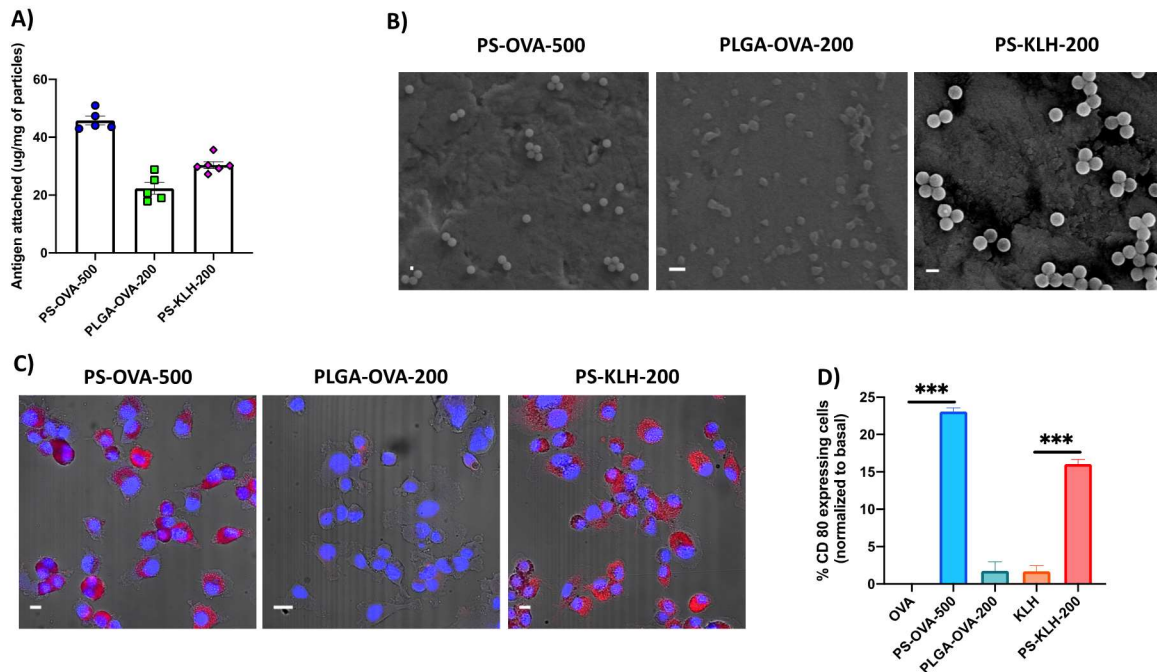


Fig. S3. Particle combinations for EDIT platform. (A) Quantification of different protein attachment to different particles using EDC chemistry. Attachment of ovalbumin to 500 nm polystyrene carboxylate and 200 nm polylactic co glycolate, and attachment of KLH to 200 nm polystyrene carboxylate. (n=6 for PS-KLH-200, n= 5 for all other groups). **(B)** Scanning electron micrographs of the different particles. Scale bar: 200 nm. **(C)** Confocal light scanning micrographs (CLSM) of dendritic cells post internalization of Alexa Fluor 647 labelled ovalbumin or KLH attached to different particles. Scale bar: 10 μ m. Blue indicates cell nuclei stained with DAPI. Red indicates AF 647 labelled ovalbumin or KLH. **(D)** Dendritic cell maturation evaluated in terms of % CD 80 expression (normalized to basal expression) (n=3 for all groups). Significantly different (Student's t test): ***: p < 0.001. Data in (A-D) are expressed as mean \pm s.e.m.

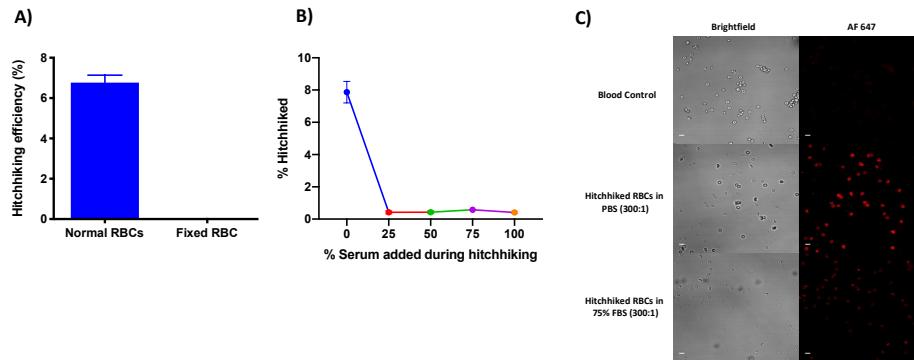


Fig. S4. Mechanistic understanding of erythrocytes-nanoparticle binding. (A) Hitchhiking efficiency change when erythrocytes are fixed indicating that physical wrapping of nanoparticles is needed to achieve proper hitchhiking. **(B)** Addition of serum during hitchhiking process affects the process, indicating that even a minimum amount of serum affects the protein-protein interactions from happening, suggesting they are important interactions governing hitchhiking. **(C)** Confocal laser scanning microscopy images of hitchhiked nanoparticles on erythrocytes. Scale bar: 10 μ m. Red color indicates Alexa Fluor 647 labelled ovalbumin. Data expressed in **(A, B)** as mean \pm s.e.m.

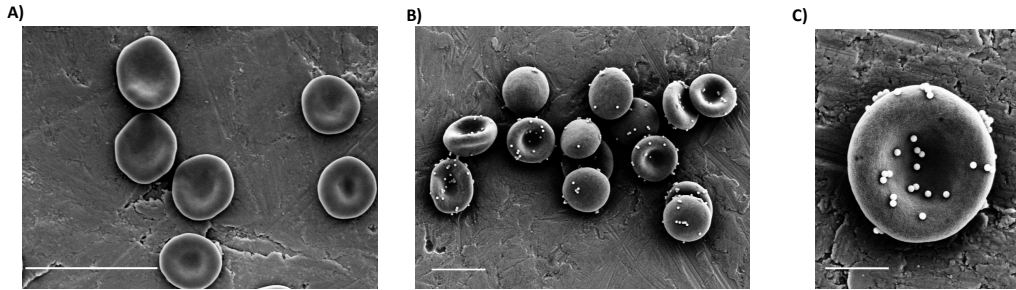


Fig. S5. Scanning electron micrographs of nanoparticles hitchhiked on erythrocytes. (A) Group of control erythrocytes. Scale bar: 10 μm . **(B)** Group of hitchhiked erythrocytes. Scale bar: 10 μm . **(C)** Single erythrocyte showing hitchhiked nanoparticles. Scale bar: 2 μm

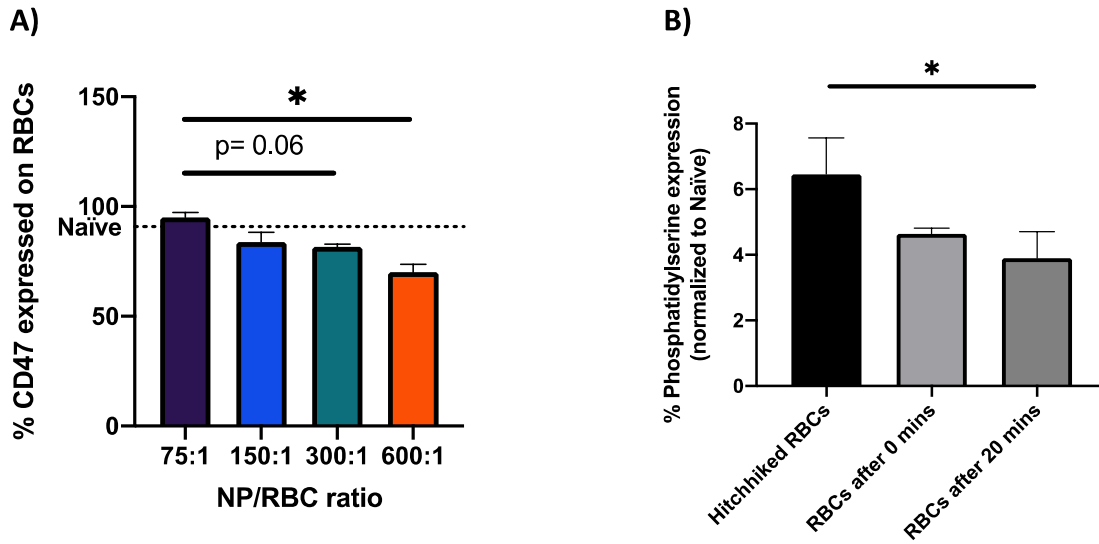


Fig. S6. Changes in the surface marker expressions on erythrocyte membranes. (A) Percentage expression of CD47 on erythrocyte membrane. Naïve cells expression indicated by dotted lines. (n=3 for all groups). Significantly different. (One-way ANOVA followed by Tukey's HSD test). *: $p < 0.05$. **(B)** Kinetics of changes in phosphatidylserine expression as normalized to the basal. Groups indicate hitchhiked erythrocytes before injection, tracked erythrocytes immediately after injection and tracked erythrocytes 20 mins after injection (when the nanoparticles are expected to be sheared off) (n=3). Significantly different. (One-way ANOVA followed by Tukey's HSD test). *: $p < 0.05$. Data expressed as mean \pm s.e.m.

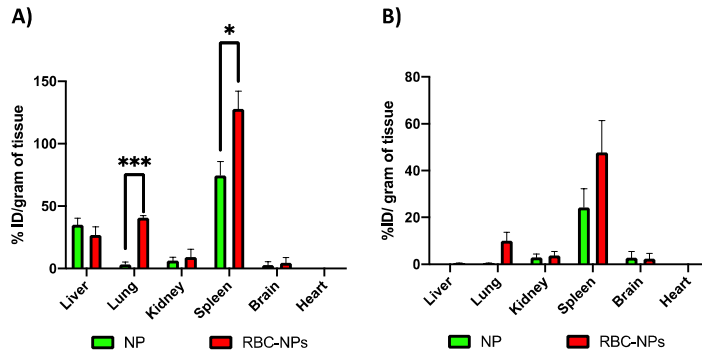


Fig. S7. Biodistribution of hitchhiked and free nanoparticles 6 h and 24 h after intravenous injections. (A) Biodistribution at 6h. (n=3 for all groups). Significantly different. (Student's t test).

*: $p < 0.05$, ***: $p < 0.001$. **(B)** Biodistribution at 24h. Data expressed as mean \pm s.e.m.

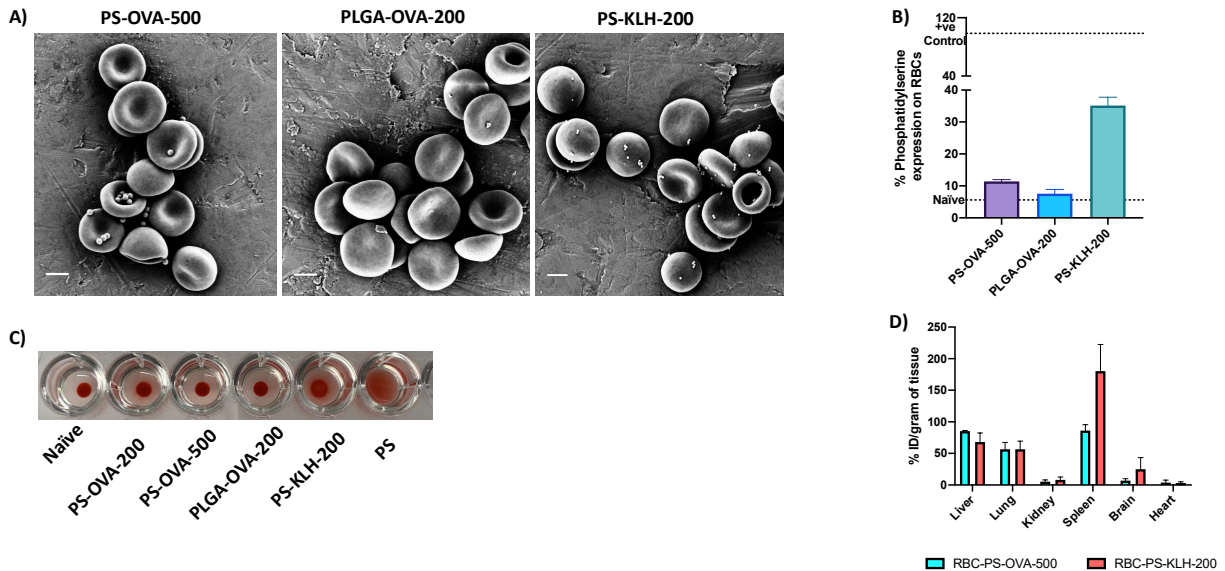


Fig. S8. Potential of EDIT to deliver different nanoparticle combinations to spleen. (A) Scanning electron micrographs of erythrocytes with hitchhiked nanoparticles (PS-OVA-500, PLGA-OVA-200, PS-KLH-200). All scale bars: 2 μ m **(B)** Erythrocyte damage caused by nanoparticles, evaluated by changes in percentage of phosphatidylserine expression, for different protein capped particles, at a nanoparticle to erythrocyte feed ratio of 300:1 (n=3 for all groups). Dotted lines indicate phosphatidyl serine expression on Naïve erythrocytes and the damaged caused by positive control (polystyrene beads). **(C)** Optical agglutination assay demonstrating damage induced by nanoparticles to erythrocytes for different protein capped particles, at a nanoparticle to erythrocyte feed ratio of 300:1. All the tested particles were similar to Naïve control as opposed to polystyrene induced matrix shaped aggregates. **(D)** Biodistribution of hitchhiked nanoparticles, 20 minutes injection, evaluated by IVIS imaging. All the hitchhiked particles showed high spleen delivery efficiency. (n=3 for all groups). Data in **(B, D)** are expressed as mean \pm s.e.m.

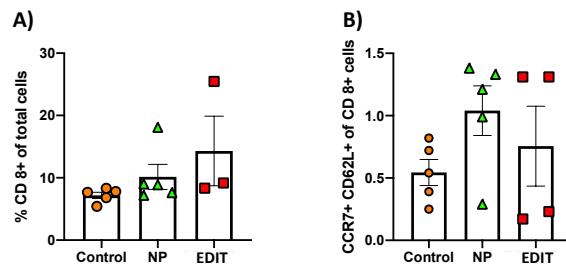


Fig. S9. Immunological consequences of enhanced delivery in the lung. (A) Quantitative analysis of CD8 + cells present in the lungs. (n=3 for EDIT, n=5 for all other groups). **(B)** Quantitative analysis of antigen experienced CCR7+CD62L+ cells in the lungs (n=4 for EDIT, n=5 for all other groups). Data in **(A, B)** are expressed as mean \pm s.e.m.

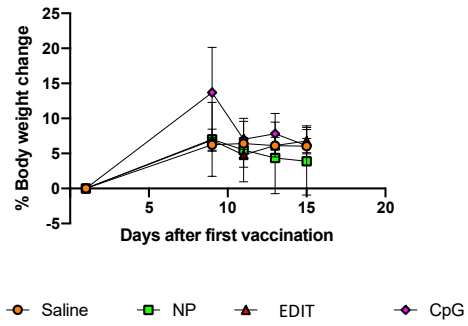


Fig. S10. Body weight change after vaccination treatments for the prophylactic studies. Data expressed as mean \pm s.e.m.